Journal of Zoo and Wildlife Medicine 47(3): 781–789, 2016

RADIOGRAPHIC THORACIC ANATOMY OF THE RED PANDA (*AILURUS FULGENS*)

Modesta Makungu, B.V.M., M.V.M., Ph.D., Wencke M. du Plessis, B.V.Sc., M. Med. Vet. (DiagIm), Ph.D., Dipl. E.C.V.D.I., Michelle Barrows, B.V.M.S., Dipl. Zoo Med. (Avian), Hermanus B. Groenewald, B.V.Sc., Ph.D., and Katja N. Koeppel, B.V.M.S., M.Sc. (Wildlife), Dipl. E.C.Z.M.

Abstract: The red panda (*Ailurus fulgens*) is classified as an endangered species by the International Union for Conservation of Nature and Natural Resources. The natural distribution of the red panda is in the Himalayas and southern China. Thoracic diseases such as dirofilariasis, hypertrophic cardiomyopathy, tracheal obstruction, lung worm infestation, and pneumonia have been reported in the red panda. The aim of this study was to describe the normal radiographic thoracic anatomy of captive red pandas as a species-specific reference for routine health examinations and clinical cases. Right lateral (RL) and dorsoventral (DV) inspiratory phase views of the thorax were obtained in 11 adult captive red pandas. Measurements were made and ratios calculated to establish reference ranges for the mean vertebral heart score on the RL (8.34 ± 0.25) and DV (8.78 ± 0.34) views and the mean ratios of the caudal vena cava diameter to the vertebral body length above tracheal bifurcation (0.67 ± 0.05) and tracheal diameter to the width of the third rib (2.75 ± 0.24). The majority of animals (10/11) had 14 thoracic vertebrae, except for one animal that had 15 thoracic vertebrae. Rudimentary clavicles were seen in 3/11 animals. The ovoid, oblique cardiac silhouette was more horizontally positioned and elongated in older animals. A redundant aortic arch was seen in the oldest animal. The trachea was seen with mineralized cartilage rings in all animals. The carina was clearly seen in the majority of animals (10/11). Variations exist in the normal radiographic thoracic anatomy of different species. Knowledge of the normal radiographic thoracic anatomy of the red panda should prove useful for routine health examinations and in the diagnosis of thoracic diseases.

Key words: *Ailurus fulgens*, anatomy, radiography, red panda, thorax.

INTRODUCTION

The red panda (*Ailurus fulgens*) is classified as an endangered species by the International Union for Conservation of Nature and Natural Resources.[18] Its natural distribution is in the Himalayas and southern China.[9] The red panda, a member of the Family Ailuridae, is closely related to procyonids, mustelids, and skunks and is a species commonly kept in zoological collections.[13] The head and body length of the red panda range from 560 mm to 625 mm.[36] The mean weight of adult males and females in captivity is 5.0 kg (range, 3.7–6.2 kg) and 4.9 kg (range, 4.2–6.0 kg), respectively.[36] The average lifespan of the red panda in captivity is 13.4 yr, whereas in the wild the lifespan ranges from 8 to 10 yr.[17]

The trachea of the red panda consists of 38 cartilage rings, and it is 4.5 inches (11.43 cm) in length and 0.5 inches (1.27 cm) in average width.[10] The cartilage rings are incomplete dorsally, as described in domestic cats and dogs.[8,24] The trachea branches into two short principal bronchi: the left and right principal bronchi. The right principal bronchus is shorter and wider than the left principal bronchus.[10] The right lung consists of four lobes (i.e., the cranial, middle, caudal, and accessory lobes). The left lung consists of two lobes (i.e., the cranial and caudal lobes).[10] The cranial lobe of the left lung is not subdivided into cranial and caudal parts, as is the case in domestic cats and dogs.[36]

Various thoracic diseases such as traumatic pericarditis, right heart failure, hypertrophic cardiomyopathy, dirofilariasis, pleuritis, tracheal obstruction, bovine tuberculosis, anthracosis, lung worm infestation, lung sarcoma, and infectious and noninfectious pneumonias (such as aspiration pneumonia, chronic fibrosing interstitial pneumo-

From the Department of Anatomy and Physiology, Faculty of Veterinary Science, University of Pretoria, Private Bag X04, Onderstepoort 0110, South Africa (Makungu, Groenewald); Ross University School of Veterinary Medicine, P.O. Box 334, Basseterre, St. Kitts, West Indies (du Plessis); Bristol Zoo Gardens, Clifton, Bristol BS8 3HA, United Kingdom (Barrows); and the Johannesburg Zoo, Private Bag X13, Parkview, Johannesburg 2122, South Africa (Koeppel). Present addresses (Makungu): Department of Veterinary Surgery and Theriogenology, Faculty of Veterinary Medicine, Sokoine University of Agriculture, P.O. Box 3020, Morogoro, Tanzania; (Koeppel): Department of Production Animal Studies–Wildlife, Faculty of Veterinary Science, University of Pretoria, Private Bag X04, Onderstepoort 0110, South Africa. Correspondence should be directed to Dr. Makungu (modesta_makungu@yahoo.com).

nia, and verminous pneumonia) have been reported in the red panda.[6,12,15,32,34,35,42]

Radiography is a noninvasive diagnostic imaging modality that is used for diagnosis of various thoracic diseases.[3,11,26,37,38] It is commonly used as the first diagnostic imaging modality for thoracic diseases in animals. Knowledge of the normal radiographic thoracic anatomy of individual species is important for accurate interpretation and diagnosis of thoracic disease.[39] The normal radiographic thoracic anatomy of companion animals is well documented, which provides a reference for diagnosis of thoracic disease.[40]

The aim of this study was to describe the normal radiographic thoracic anatomy of captive red pandas as a species-specific reference for routine health examinations and clinical cases. To the best of the authors' knowledge this has not been published previously.

MATERIALS AND METHODS

Animals

Eleven adult captive red pandas from the Johannesburg Zoo, South Africa, without clinical evidence of thoracic disease were imaged in this study. The age, body weight, and sex of the red pandas were recorded. This study was approved by the Animal Use and Care Committee of the University of Pretoria and Johannesburg Zoo Research Committee.

Radiography

Radiography of the thorax was performed under general anesthesia during annual health examinations. Animals were fasted for 8–12 hr, but water was given ad libitum until shortly before anesthesia. Anesthesia was induced using medetomidine hydrochloride [Domitor, Pfizer Laboratories (Pty) Ltd., Sandton, 2196, South Africa; mean dosage, 0.08 ± 0.01 mg/kg; range, 0.05–0.09 mg/kg i.m.] and ketamine hydrochloride [Kyron Laboratories (Pty) Ltd., Benrose, 2094, South Africa; mean dosage, 7.4 ± 0.94 mg/kg; range, 5.4–8.8 mg/kg i.m.]. Animals were intubated and anesthesia maintained using isoflurane [Isofor, Safeline Pharmaceuticals (Pty) Ltd., Roodepoort, 1709, South Africa; percentage range, 1–2.5%].

In 10 animals, a table-top technique was used and radiography was performed using an EVA-HF525 (Comed Medical System Co. Ltd., 58 Hakdong, Kyunggi, Korea) x-ray machine. A source to image distance (SID) of 95 cm was used, with a kVp range of 46 to 48 and 1.25 mAs. In 9/10 animals, images were obtained by a film-screen system. In the remaining animal (1/10), computed radiography (CR) (Vita LE, Carestream Health Inc., Rochester, New York 14608, USA) was used. For the film-screen system, an automatic x-ray film processor model CP-345 (ELK Corporation, Tokyo 113–0034, Japan) was used with medium-speed screen-type films (Fujifilm Corporation, Tokyo 107–0052, Japan) in combination with RAREX green regular intensifying screens (Okamoto manufacturing Co. Ltd., Tokyo 169–0051, Japan). Radiographic films were digitalized using a digital camera (CANON 5DMARK2, Canon Inc., Tokyo 146–8501, Japan).

In 1/11 animals, a Siemens polymat 50 x-ray machine (Siemens, 91052 Erlangen, Germany) was used at kVp and mAs values of 96 and 2, respectively. Images were obtained using a Fuji Axim FCR Capsula XL (Fujifilm Corporation, Tokyo 107–0052, Japan) CR system. A bucky table grid of 8 : 1 was used at an SID of 107 cm. In all animals, right lateral (RL) and dorsoventral (DV) inspiratory phase views of the thorax were taken without positive-pressure ventilation. Radiography was performed immediately after a maintenance plane of anesthesia was established. Prior to radiography animals were positioned in lateral recumbency.

Radiographic evaluation

The visibility, shape, and location of the thoracic organs were recorded. The depth of the thorax was measured on the RL view (Fig. 1) from the dorsocaudal border of the seventh sternebra to the closest edge of the vertebral column.[25] The closest edge of the vertebral column was the cranioventral edge of the cranial endplate of thoracic vertebra 8 (Fig. 1) and 9 in an animal with 14 and 15 thoracic vertebrae, respectively. The width of the thorax was measured on the DV view (Fig. 2) as the maximum distance between the left and right pleural surfaces of the eighth ribs.[25]

The lengths of thoracic vertebral bodies and sternebrae, excluding the manubrium sterni and xiphoid process (Fig. 1), were measured on the RL view from the midpoint of the cranial edge of the cranial endplate to the midpoint of the caudal edge of the caudal endplate.[31] The heights of thoracic vertebral bodies and sternebrae (Fig. 1) were measured on the RL view along a line that extended between the cranioventral and craniodorsal borders of the vertebral body and sternebra, respectively.[31]

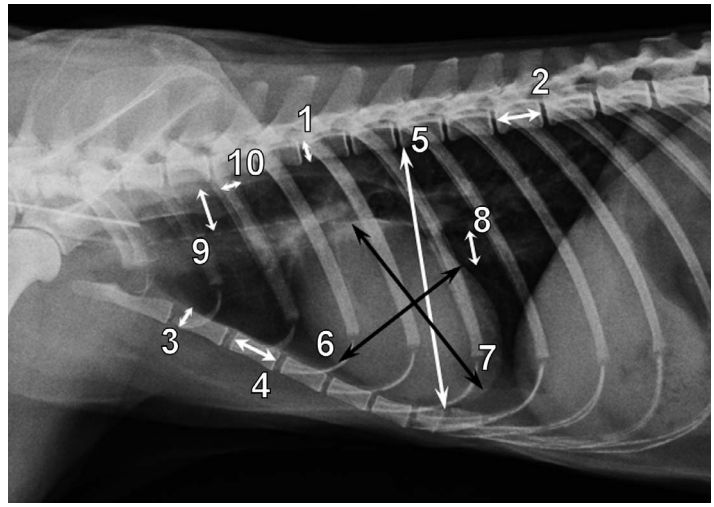

Figure 1. Right lateral thoracic radiograph of a 10-yr-old male (5.5-kg) red panda illustrating radiographic measurements: Vertebral body height (1), vertebral body length (2), height of sternebra (3), length of sternebra (4), thoracic depth (5), cardiac silhouette short-axis measurement (6), cardiac silhouette long-axis measurement (7), caudal vena cava diameter (8), tracheal diameter (9), and width of the third rib (10).

The vertebral heart score (VHS) was measured on the RL and DV views as previously described in domestic cats.[25] Cardiac long axis and cardiac short axis measurements on the RL (Fig. 1) and DV (Fig. 2) views were used to calculate the VHS on the RL and DV views as well as cardiothoracic ratios.[25,31]

The greatest diameter of the caudal vena cava (CVC) not overlapping the cardiac silhouette or diaphragm was measured on the RL view perpendicular to the long axis of the CVC (Fig. 1).[22] The diameter of the CVC was also compared to the length of the thoracic vertebral body above the tracheal bifurcation.[22] The width of the craniodorsal mediastinum was measured at the level of the third rib head on the DV view (Fig. 2).[41]

The ratio of the tracheal diameter (TD) to the width of the third rib was calculated on the RL view as previously described.[14] The TD was measured at the level of the second intercostal space, whereas the width of the third rib was measured at the proximal one-third (Fig. 1).[14] The location of the carina with respect to intercostal space (ICS) and thoracic vertebra was determined on the RL view. All radiographic measurements were not compensated for magnification.

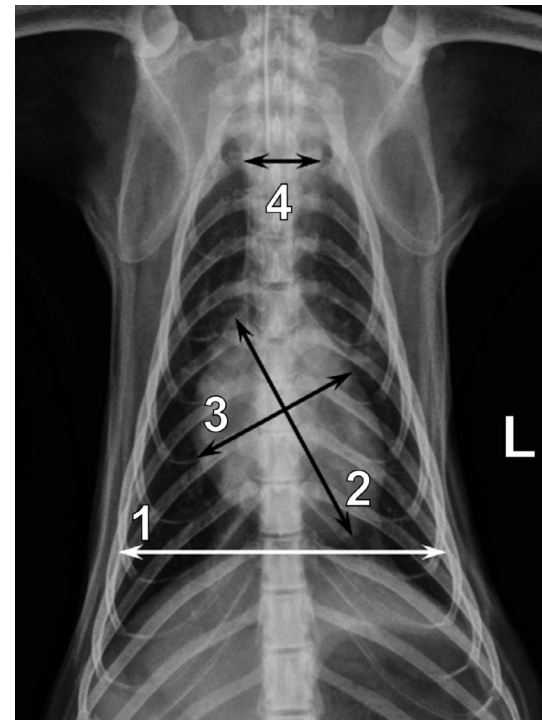

Figure 2. Dorsoventral thoracic radiograph of a 10-yr-old male (5.5-kg) red panda illustrating radiographic measurements: Thoracic width (1), cardiac silhouette long-axis measurement (2), cardiac silhouette short-axis measurement (3), and width of the craniodorsal mediastinum (4). L = left.

Data analysis

Data were analyzed using Stat View® statistical package (SAS Institute, Cary, North Carolina 27513, USA). Mean, standard deviation, and range were calculated. Student *t*-test was used to

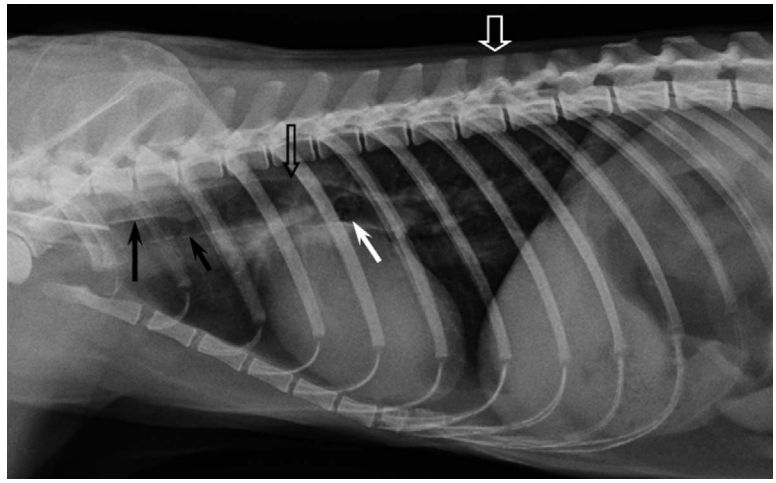

Figure 3. Right lateral thoracic radiograph of a 10-yr-old male (5.5-kg) red panda. Note the short spinous processes of the thoracic vertebrae and anticlinal thoracic vertebra No. 10 (open white arrow). The sternum is fairly straight, with eight sternebrae. The trachea with mineralized cartilage rings (short black arrow) is aligned almost parallel to the thoracic spine and diverges from the thoracic spine from thoracic vertebra 6 (open black arrow) caudally. Note also the superimposition of the caudal borders of the scapulae to the trachea (long black arrow) and clearly visible carina in the fifth intercostal space (white arrow). The cardiac silhouette is ovoid and obliquely positioned, occupying not more than 3.5 intercostal spaces.

compare the mean age and weight between male and female animals as well as the means of VHS on RL view versus DV view. Statistical significance was accepted at $P \leq 0.05$. Data are expressed as mean ± standard deviation (SD).

RESULTS

The age of animals ranged from 1.4 to 14.3 yr (mean, 5.9 ± 4.6 yr). The minimum weight of the animals was 3.7 kg, and the maximum weight of the animals was 6.0 kg (mean, 4.7 ± 0.7 kg). Of the 11 animals, six were females and five were males. There was no significant difference ($P = 0.38$) in the mean age between male and female animals. The mean weight of male animals (5.06 ± 0.92 kg) was higher than that of the female animals (4.41 ± 0.41 kg), although this difference was not statistically significant ($P = 0.15$).

Musculoskeletal system

Of the 11 animals, 10 had 14 thoracic vertebrae (Fig. 3), whereas one animal (female) had 15 thoracic vertebrae. Animals with 14 thoracic vertebrae had 14 pairs of ribs, of which the last two pairs were floating (Fig. 3). The animal with 15 thoracic vertebrae had 15 pairs of ribs, of which the last three pairs were floating. The spinous processes of thoracic vertebrae were short and decreased in length from cranial to caudal (Fig. 3). The anticlinal vertebra was thoracic vertebra 11 (T11) in 10/11 animals and T10 in one animal (Fig. 3). The animal with T10 as its anticlinal vertebra had 14 thoracic vertebrae (Fig. 3). Generally, the size of thoracic vertebral bodies increased from cranial to caudal (Fig. 3).

The sternum was fairly straight (Figs. 3, 4). It consisted of eight sternebrae, including the manubrium sterni and xiphoid process (10/11) (Figs. 3, 4A), except in one animal, in which it consisted of seven sternebrae (Fig. 4B). In the animal with seven sternebrae the mineralized xiphoid process was not seen (Fig. 4B). The mineralized xiphoid process was very small (Fig. 4A) or was not seen at all (Fig. 4B) in young animals. The length of the sternebrae decreased from cranial to caudal (Fig. 4). Rudimentary clavicles were seen in 3/11 animals (Fig. 5). Of the three animals with rudimentary clavicles, in one animal it was unilateral in the left shoulder joint. Radiographic measurements and findings are reported in Tables 1–3.

Cardiovascular system

On the RL view, the cardiac silhouette was ovoid and obliquely positioned, and the long axis formed an acute angle with the thoracic spine (Fig. 3). The oblique cardiac silhouette was more horizontally positioned and elongated in older animals. The cranial and caudal borders of the cardiac silhouette were located at the third rib and

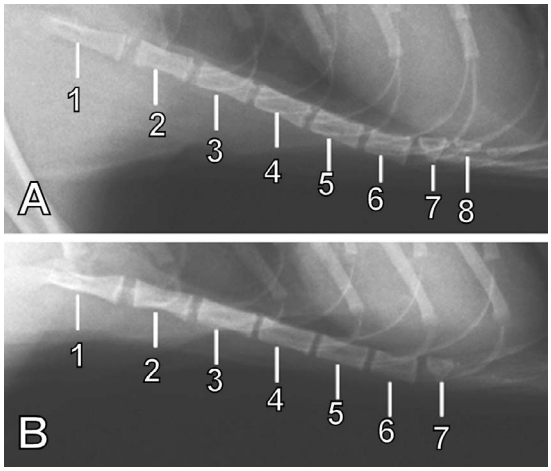

Figure 4. Close-up of right lateral thoracic radiographs of the sternum of 1.4-yr-old male (5.6-kg) (**A**) and female (4-kg) (**B**) red pandas. Note the visibility of a small mineralized xiphoid process in (**A**) and lack of visibility of the mineralized xiphoid process in (**B**). Manubrium sterni (1), second sternebra (2), third sternebra (3), fourth sternebra (4), fifth sternebra (5), sixth sternebra (6), seventh sternebra (7), and xiphoid process (8).

sixth intercostal space, respectively, in 8/11 animals (Fig. 3). In the remaining three animals, the cranial and caudal borders of the cardiac silhouette were located at the level of the fourth and seventh ribs, respectively. The size of the cardiac silhouette ranged from 3.0 to 3.5 intercostal spaces (Fig. 3). Cardiodiaphragmatic contact was seen in only one animal.

On the DV view, the cardiac silhouette was ovoid, and the apex was located in the left hemithorax (Fig. 5). Cardiodiaphragmatic contact was seen in 8/11 animals (Fig. 5). In the heaviest animal (6 kg), the cardiac silhouette was rounded, and there was extensive cardiodiaphragmatic contact (Fig. 6). The cardiac silhouette was elongated in older animals. The mean VHS measured on the DV view (8.78 ± 0.34) was significantly larger ($P = 0.0002$) than that measured on the RL view (8.34 ± 0.25) (Table 3).

The aorta was variably visible on the RL and DV views. The dorsal border of the descending aorta was not clearly seen (2/11) (Fig. 3) or was not seen at all (9/11); however, the left lateral border was clearly seen in all animals (Fig. 5). The aortic arch was elongated (redundant) in one 14.3-yr-old animal that created a left bulging contour on the DV view. The CVC was clearly seen on the RL view in all animals (Fig. 3) but was only clearly seen in 3/11 animals on the DV view.

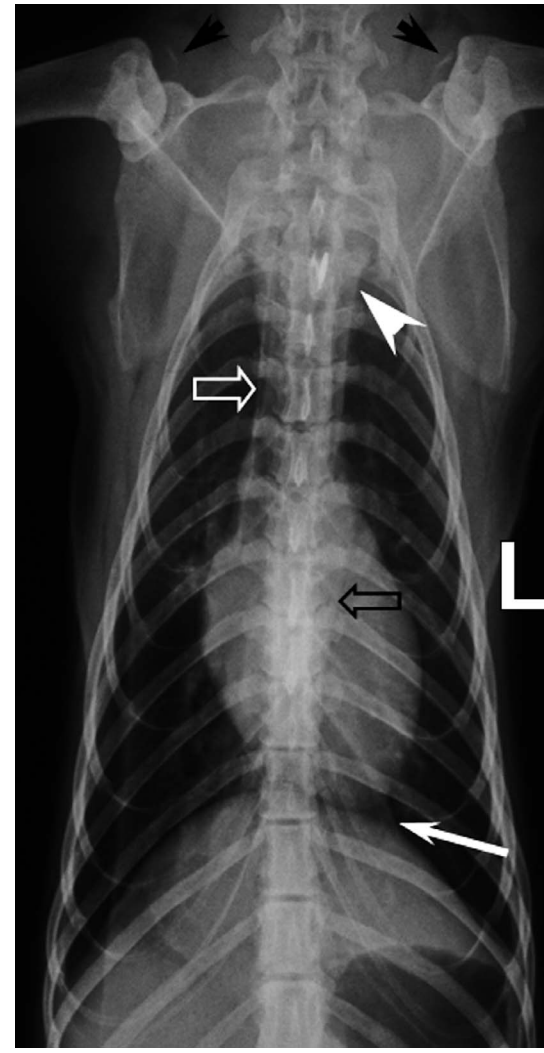

Figure 5. Dorsoventral thoracic radiograph of a 1.4-yr-old (5.6-kg) male red panda. Note the presence of the rudimentary clavicles (black arrows). The cardiac silhouette is ovoid and the apex is located in the left hemithorax. Note also the presence of minimal cardiodiaphragmatic contact. The trachea is positioned slightly to the right of the spine (open white arrow). The craniodorsal mediastinum is wider than the thoracic spine (white arrow head). The left margin of the descending aorta and the caudoventral mediastinal reflection are indicated by an open black arrow and a white arrow, respectively. L = left.

Respiratory system

On the RL view, the trachea was seen with mineralized cartilage rings in all animals (Fig. 3). It was aligned parallel to the thoracic spine and diverged ventrally from the thoracic spine from the level of the sixth or seventh thoracic vertebra

Table 1. Radiographic measurements (cm) of thoracic vertebrae in captive red pandas (*Ailurus fulgens*) not compensated for magnification.[a]

Vertebra	Variable	No.	Mean ± SD (cm)	Range (cm)
T1	Length	11	1.06 ± 0.06	1.00–1.15
	Height	11	0.56 ± 0.05	0.50–0.60
T2	Length	11	1.17 ± 0.05	1.10–1.25
	Height	11	0.60 ± 0.06	0.50–0.70
T3	Length	11	1.21 ± 0.06	1.10–1.30
	Height	11	0.65 ± 0.07	0.60–0.80
T4	Length	11	1.20 ± 0.05	1.10–1.30
	Height	11	0.66 ± 0.05	0.60–0.70
T5	Length	11	1.22 ± 0.06	1.10–1.30
	Height	11	0.66 ± 0.05	0.60–0.70
T6	Length	11	1.26 ± 0.05	1.20–1.30
	Height	11	0.72 ± 0.06	0.60–0.80
T7	Length	11	1.26 ± 0.05	1.20–1.30
	Height	11	0.74 ± 0.05	0.70–0.80
T8	Length	10	1.27 ± 0.05	1.20–1.30
	Height	10	0.74 ± 0.05	0.70–0.80
T9	Length	10	1.29 ± 0.07	1.20–1.40
	Height	10	0.78 ± 0.08	0.70–0.90
T10	Length	10	1.36 ± 0.07	1.20–1.45
	Height	10	0.81 ± 0.09	0.70–0.90
T11	Length	10	1.43 ± 0.09	1.30–1.55
	Height	10	0.92 ± 0.35	0.70–1.90
T12	Length	10	1.52 ± 0.09	1.40–1.65
	Height	10	0.82 ± 0.12	0.70–0.90
T13	Length	10	1.60 ± 0.09	1.40–1.75
	Height	10	0.86 ± 0.08	0.75–1.00
T14	Length	10	1.73 ± 0.11	1.50–1.85
	Height	10	0.99 ± 0.33	0.80–1.90
T15	Length	1	1.80 ± 0.00	1.80–1.80
	Height	1	0.80 ± 0.00	0.80–0.80

[a] T indicates thoracic vertebra.

Table 2. Radiographic measurements (cm) of sternebrae in captive red pandas (*Ailurus fulgens*) not compensated for magnification.[a]

Sternebra	Variable	No.	Mean ± SD (cm)	Range (cm)
S2	Length	11	1.48 ± 0.12	1.30–1.65
	Height	11	0.58 ± 0.06	0.50–0.70
S3	Length	11	1.46 ± 0.08	1.40–1.60
	Height	11	0.60 ± 0.08	0.50–0.70
S4	Length	11	1.41 ± 0.09	1.30–1.60
	Height	11	0.56 ± 0.05	0.50–0.60
S5	Length	11	1.32 ± 0.08	1.20–1.45
	Height	11	0.57 ± 0.05	0.50–0.60
S6	Length	11	1.19 ± 0.08	1.10–1.30
	Height	11	0.56 ± 0.08	0.40–0.70
S7	Length	9	0.92 ± 0.16	0.70–1.10
	Height	9	0.53 ± 0.11	0.40–0.70

[a] S indicates sternebrae.

caudally to the carina in six and five animals, respectively (Fig. 3). The caudal borders of the scapulae were superimposed over the trachea (Fig. 3). The mean ratio of the tracheal diameter to the width of the third rib was 2.75 ± 0.24 (Table 3). The carina was clearly seen (Fig. 3) in the majority of animals (10/11). The mean location of the carina with respect to ICS and vertebra was 5.27 ± 0.47 and 7.27 ± 0.47, respectively. In most animals (7/11), the pulmonary cupula ended at the caudal border of the first rib (Fig. 3) and rarely at the first intercostal space (3/11) or cranial border of the first rib (1/11). The diaphragmatic crura were frequently seen to be parallel (6/11) and were less frequently superimposed (3/11) or diverged dorsally (2/11) (Fig. 3).

On the DV view, the trachea was running slightly to the right of the spine in all animals (Fig. 5). The left and right pulmonary cupulae did not extend cranially beyond the second rib (Fig. 5). In all animals the craniodorsal mediastinum exceeded the width of the spine (Figs. 5, 6). The cranioventral mediastinal reflection was not seen in any animal. The caudoventral mediastinal reflection was seen in 6/11 animals (Fig. 5). A mild alveolar lung pattern was seen in one animal in the right hemithorax adjacent to the right cardiac margin (Fig. 6). Pleural fissure lines were not observed in any animal. The diaphragm appeared as a single dome in all animals (Figs. 5, 6).

Other findings

Three animals (two females and one male) older than 9 yr of age had multiple areas of lateral and ventral spondylosis deformans, with the caudal thoracic vertebrae being severely affected. The esophagus and thoracic lymph nodes were not seen.

DISCUSSION

Thoracic anatomic structures of clinical importance in red pandas were seen and evaluated radiographically. The mean ratio of thoracic depth to thoracic width obtained in this study (0.82) indicates a normal thoracic conformation similar to that of the coati (*Nasua nasua*) (1.05).[4,27] The number of thoracic vertebrae observed in the majority of red pandas (14) is also similar to that observed in the coati. Most coati had 14 pairs of ribs, consistent with 14 thoracic vertebrae.[28] In this study the anticlinal vertebra was mostly T11, which is similar to what is observed in the domestic cat and dog.[23] Variation in the number of ribs (14 to 15) and the presence of 14 pairs of ribs in the majority of animals in this study have also been reported in the coati.[28] The presence of

Table 3. Radiographic findings and measurements of the thorax not compensated for magnification in captive red pandas (*Ailurus fulgens*).[a]

Variable	No.	Mean ± SD	Range
TDp (cm)	11	7.53 ± 0.38	7.00–8.10
TW (cm)	11	9.17 ± 0.56	8.20–10.10
TDp : TW	11	0.82 ± 0.05	0.75–0.91
Anticlinal vertebra	11	10.91 ± 0.30	10.00–11.00
CLA (RL) (cm)	11	6.71 ± 0.35	6.20–7.50
CSA (RL) (cm)	11	4.56 ± 0.33	4.00–5.00
CLA (DV) (cm)	11	7.08 ± 0.24	6.70–7.30
CSA (DV) (cm)	11	4.79 ± 0.30	4.20–5.30
CLA(RL) : TDp	11	0.89 ± 0.04	0.84–0.93
CSA (RL) : TDp	11	0.61 ± 0.04	0.55–0.67
CLA (DV) : TW	11	0.77 ± 0.04	0.70–0.83
CSA (DV) : TW	11	0.53 ± 0.05	0.45–0.60
VHS (RL)	11	8.34 ± 0.25	8.00–8.90
VHS (DV)	11	8.78 ± 0.34	8.30–9.60
CVC diameter (cm)	11	0.85 ± 0.06	0.80–0.95
CVC : VL	11	0.67 ± 0.05	0.62–0.75
MDWd (cm)	11	2.34 ± 0.16	2.00–2.50
Carina			
ICS	11	5.27 ± 0.47	5.00–6.00
Vertebra	11	7.27 ± 0.47	7.00–8.00
TD (cm)	11	1.35 ± 0.13	1.1–1.5
Third rib width (cm)	11	0.49 ± 0.02	0.45–0.50
TD: Third rib width	11	2.75 ± 0.24	2.2–3.0
Cranial crus (RL)	11	14.06 ± 0.69	12.6–14.7
Diaphragm (DV)	11	11.66 ± 0.46	11.00–12.40

[a] TDp indicates thoracic depth; TW, thoracic width; CLA, cardiac long axis; CSA, cardiac short axis; RL, right lateral; DV, dorsoventral; VHS, vertebral heart score; CVC, caudal vena cava; VL, vertebral body length; MDWd, mediastinal width; ICS, intercostal space; TD, tracheal diameter.

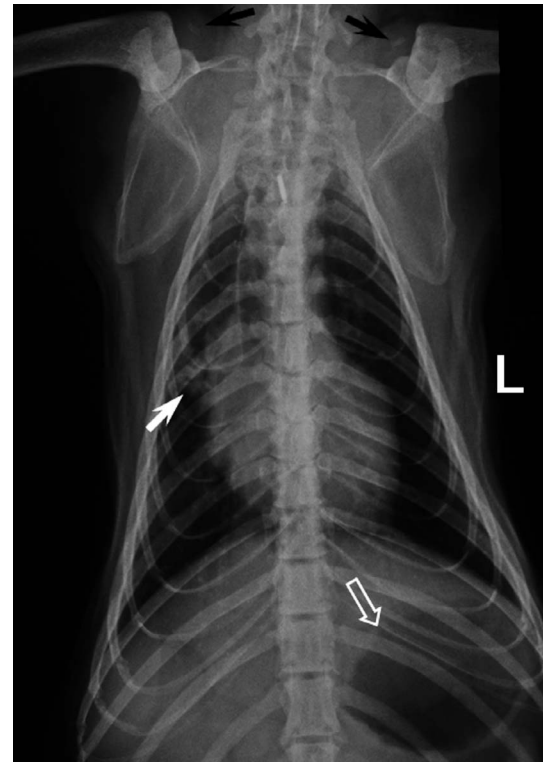

Figure 6. Dorsoventral thoracic radiograph of an 8-yr-old (6-kg) male red panda. The cardiac silhouette is rounded and there is extensive cardiodiaphragmatic contact. Note the presence of a mild alveolar lung pattern (white arrow) in the right hemithorax adjacent to the right cardiac margin as a result of gravity-dependent atelectasis. Note also the presence of gas in the gastric fundus (open white arrow). The clavicles are indicated by black arrows. L = left.

two pairs of floating ribs is similar to that seen in the domestic cat.[23] In this study, the majority of red pandas (10/11) had eight sternebrae, which is similar to findings in the domestic cat and dog.[23] The fairly straight sternum resembles that of the coati.[28]

The presence of rudimentary clavicles in some red pandas is similar to that seen in domestic dogs.[5,29] The rudimentary clavicles should not be misinterpreted as dystrophic mineralization as a result of neoplasia, granulomas, or abscesses.[1] Multiple areas of ventral and lateral thoracic spondylosis are considered incidental findings. Similar changes have been observed in domestic cats and dogs and are less frequent and milder in the domestic cat.[20,21]

The mean VHS of the red panda obtained from RL (8.34 ± 0.25) and DV (8.78 ± 0.34) views is intermediate between the values reported in the domestic cat (RL: 7.5 ± 0.3; DV: 8.1 ± 0.45) and dog (RL: 9.7 ± 0.5; DV: 10.2 ± 1.45).[4,25] However, it is slightly lower than the reported mean value in the adult coati.[27] The significant difference in the mean VHS obtained on the RL and DV views in this study has also been observed in the domestic cat and dog.[4,25] Measuring the VHS on the RL view in heavy red pandas is recommended as a result of the change in the shape of the cardiac silhouette on the DV view, in which it may be difficult to define the cardiac borders precisely.

The oblique position of the cardiac silhouette in this species is similar to that observed in the domestic cat.[2] Further, the more horizontally positioned and elongated cardiac silhouette and redundant aortic arch, which were seen in older animals in this study, have also been observed in older domestic cats.[30] These changes are not pathologic and are most likely associated with age-related changes in thoracic conformation.[19]

Similar changes have also been reported in older captive maned wolves (*Chrysocyon brachyurus*).[7]

Mineralization of the tracheal rings, which was observed in all animals, should not be misinterpreted as an aging change or an incidental finding. It is a normal feature in this species. The presence of mineralization of the tracheal rings in this species is similar to that seen in the coati.[28] The mean ratio of the tracheal diameter to the width of the third rib obtained in this study (2.75 ± 0.24) was higher than the reported mean in Persian (1.71) and domestic shorthair (1.59) cats.[14] The superimposition of the scapulae over the trachea on the RL view should not be misinterpreted as redundancy of the dorsal tracheal membrane since the tracheal rings of the red panda are also incomplete dorsally, as is the case with the domestic cat and dog.[40]

The parallel alignment of the trachea with the thoracic spine on the RL view is a normal feature in this species and should not be misinterpreted as dorsal displacement of the trachea as a result of cardiomegaly or a mediastinal mass.[16] Parallel alignment of the trachea with the thoracic spine has also been seen in the normal Dachshund and Welsh corgi.[40] The location of the trachea slightly to the right of the spine on the DV view is similar to that seen in the domestic dog.[16,40] The lung pattern (mild alveolar), which was observed in one animal, is believed to be the result of RL recumbency causing gravity-dependent atelectasis. This is due to the fact that the lung pattern occurred in the heaviest animal and was located in the right hemithorax. Furthermore, none of the animals used in this study had evidence of thoracic disease on clinical examination. Positive-pressure ventilation improves overall lung contrast in general anesthetized animals; however, it was not used in this study.[33]

CONCLUSIONS

Variations exist in the normal radiographic anatomy of the thorax of different species. Knowledge of the normal radiographic anatomy of the red panda thorax should prove useful in the diagnosis of thoracic disease in this species.

Acknowledgments: The authors would like to thank the Organization for Women in Science for the Developing World, Swedish International Development Cooperation Agency, University of Pretoria, and Johannesburg Zoo for supporting this study. Dr. Georgina Cole, Ms. Fania Mohlala, and the sisters and animal handlers of the Johannesburg Zoo and Onderstepoort Veterinary Academic Hospital are acknowledged for their assistance during radiography. Mrs. Charmaine Vermeulen and Mrs. Wilma Olivier of the University of Pretoria are acknowledged for their assistance in photography and administrative work, respectively.

LITERATURE CITED

1. Barr F. Soft tissues. In: Barr FJ, Kirberger RM (eds.). BSAVA canine and feline musculoskeletal imaging. 1st ed. Gloucester (United Kingdom): BSAVA; 2006. p. 1–8.

2. Buchanan JW. Vertebral scale system to measure heart size in radiographs. Vet Clin North Am Small Anim Pract. 2000;30:379–393.

3. Buchanan JW. Tracheal signs and associated vascular anomalies in dogs with persistent right aortic arch. J Vet Intern Med. 2004;18:510–514.

4. Buchanan JW, Bücheler J. Vertebral scale system to measure canine heart size in radiographs. J Am Vet Med Assoc. 1995;206:194–199.

5. Cerny H, Cizinauskas S. The clavicle of newborn dogs. Acta Vet Brno. 1995;64:139–145.

6. Delaski KM, Ramsay E, Gamble KC. Retrospective analysis of mortality in the North American captive red panda (*Ailurus fulgens*) population, 1992–2012. J Zoo Wildl Med. 2015;46:779–788.

7. Estrada AH, Gerlach TJ, Schmidt MK, Siegal-Willott JL, Atkins AL, Van Gilder J, Citino SB, Padilla LR. Cardiac evaluation of clinically healthy captive maned wolves (*Chrysocyon brachyurus*). J Zoo Wildl Med. 2009;40:478–486.

8. Evans HE, de Lahunta A. The respiratory system. In: Evans HE, de Lahunta A (eds.). Miller's anatomy of the dog. 4th ed. St. Louis (MO): Elsevier Saunders; 2013. p. 338–360.

9. Fisher RE, Adrian B, Barton M, Holmgren J, Tang SY. The phylogeny of the red panda (*Ailurus fulgens*): evidence from the forelimb. J Anat. 2009;215:611–635.

10. Flower WH. On the anatomy of *Ailurus fulgens*. In: Proc Zool Soc London; 1870. p. 747–795.

11. Fossum TW, Boudrieau RJ, Hobson HP. Pectus excavatum in eight dogs and six cats. J Am Anim Hosp Assoc. 1989;25:595–605.

12. Gardner HM. Case: hypertrophic cardiomyopathy in a lesser panda. In: Proc Am Assoc Zoo Vet; 1985. p. 76.

13. Groves C. The taxonomy and phylogeny of *Ailurus*. In: Glatston A (ed.). Red panda biology and conservation of the first panda. London (United Kingdom): Academic Press; 2011. p. 101–124.

14. Hammond G, Geary M, Coleman E, Gunn-Moore D. Radiographic measurements of the trachea in domestic shorthair and Persian cats. J Feline Med. 2011;13:881–884.

15. Harwel G, Craig TM. Dirofilariasis in a red panda. J Am Vet Med Assoc. 1981;179(11):1258.

16. Hayward N, Schwarz T, Weisse C. The trachea. In: Schwarz T, Johnson V (eds.). BSAVA manual of canine and feline thoracic imaging. Gloucester (United Kingdom): BSAVA; 2008. p. 213–227.

17. Heath T, Platnick J. "*Ailurus fulgens*" [Internet]. c2014 [cited 1 April 2016]. Available from http://www.animaldiversity.org/accounts/Ailurus_fulgens-2008

18. IUCN. IUCN red list of threatened species; Version 2015–4 [cited 07 June 2016]. Available from http://www.iucnredlist.org/

19. Johnson V, Hansson K, Maï W, Dukes-McEwan J, Lester N, Schwarz T, Chapman P, Morandi F. The heart and major vessels. In: Schwarz T, Johnson V (eds.). BSAVA manual of canine and feline thoracic imaging. Gloucester (United Kingdom): BSAVA; 2008. p. 86–176.

20. Kranenburg HC, Meij BP, van Hofwegen EML, Voorhout G, Slingerland LI, Picavet P, Hazewinkel HAW. Prevalence of spondylosis deformans in the feline spine and correlation with owner-perceived behavioral changes. Vet Comp Orthop Traumatol. 2012;25:217–223.

21. Kranenburg HC, Voorhout G, Grinwis GCM, Hazewinkel HAW, Meij BP. Diffuse idiopathic skeletal hyperostosis (DISH) and spondylosis deformans in purebred dogs: a retrospective radiographic study. Vet J. 2011;190:e84–e90.

22. Lehmkuhl LB, Bonagura JD, Biller DS, Hartman WM. Radiographic evaluation of caudal vena cava size in dogs. Vet Radiol Ultrasound. 1997;38:94–100.

23. Liabrés-Díaz F, Petite A, Saunders J, Schwarz T. The thoracic boundaries. In: Schwarz T, Johnson V (eds.). BSAVA manual of canine and feline thoracic imaging. Gloucester (United Kingdom): BSAVA; 2008. p. 340–376.

24. Light GS. Respiratory system. In: Hudson C, Hamilton WP (eds.). Atlas of feline anatomy for veterinarians. Philadelphia (PA): W. B. Saunders Co.; 1993. p. 135–148.

25. Litster AL, Buchanan JW. Vertebral scale system to measure heart size in radiographs of cats. J Am Vet Med Assoc. 2000;216:210–214.

26. Lobetti RG, Milner R, Lane E. Chronic idiopathic pulmonary fibrosis in five dogs. J Am Anim Hosp Assoc. 2001;37:119–127.

27. Martini AC, Meireles YS, Monzem S, Vanconcelos LP, Turbino NCMR, Dahroug MAA, Farias D, Néspoli PB, Gonçalves GF, Souza RL, Guimarães LD. Avaliação radiográfica da silhueta cardíaca, pelo método VHS (Vertebral Heart Size), de quatis (*Nasua nasua*, Linnaeus 1766) jovens e adultos mantidos em cativeiro. [Radiographic evaluation of the cardiac silhouette using the VHS method (vertebral heart score) in young and adult coatis (*Nasua nasua*, Linneaus 1766) living in captivity]. Semin Ciênc Agrár. [Semin Agri Sci]. 2013;34:3823–3830.

28. Martins GS, Lopes ER, Taques IIG, Correia CY, Meireles YS, Turbino NCMR, Guimarães LD, Néspoli PB. Aspectos da morfologia radiográfica do esqueleto, tórax e abdome do quati (*Nasua nasua* Linnaeus, 1766). [Radiographic morphology of the skeleton, thorax and abdomen of coati (*Nasua nasua* Linnaeus, 1766). Pesq Vet Bras. [Braz J Vet Res]. 2013;33:1137–1143.

29. McCarthy PH, Wood AK. Anatomic and radiologic observations of the clavicle of adult dogs. Am J Vet Res. 1988;49:956–959.

30. Moon ML, Keene BW, Lessard P, Lee J. Age related changes in the feline cardiac silhouette. Vet Radiol Ultrasound. 1993;34:315–320.

31. Nelson NC, Mattoon JS, Anderson DE. Radiographic appearance of the thorax of clinically normal alpaca crias. Am J Vet Res. 2011;72:1439–1448.

32. Patterson-Kane JC, Gibbons LM, Jefferies R, Morgan ER, Wenzlow N, Redrobe SR. Pneumonia from *Angiostrongylus vasorum* infection in a red panda (*Ailurus fulgens fulgens*). J Vet Diagn Invest. 2009;21:270–273.

33. Phair K, West G, Biller D. The use of intermittent positive pressure ventilation to differentiate pneumonia from atelectasis during anesthesia in a red panda (*Ailurus fulgens*). J Zoo Wildl Med. 2010;41:739–741.

34. Philippa J, Ramsay E. Captive red panda medicine. In: Glatston AR (ed.). Red panda biology and conservation of the first panda. London (United Kingdom): Academic Press; 2011. p. 271–285.

35. Preece B. Red panda pathology. In: Glatston AR (ed.). Red panda biology and conservation of the first panda. London (United Kingdom): Academic Press; 2011. p. 287–302.

36. Roberts MS, Gittleman JL. *Ailurus fulgens*. Mamm Species. 1984;222:1–8.

37. Sullivan M, Lee R. Radiological features of 80 cases of diaphragmatic rupture. J Small Anim Pract. 1989;30:561–566.

38. Suter PF. The radiographic diagnosis of canine and feline heart disease. Compend Contin Ed Small Anim. 1981;3:441–454.

39. Thrall DE. Introduction to radiographic interpretation. In: Thrall DE (ed.). Textbook of veterinary diagnostic radiology. St. Louis (MO): Saunders Elsevier; 2013. p. 74–86.

40. Thrall DE, Robertson ID. Atlas of normal radiographic anatomy and anatomic variants in the dog and cat. St. Louis (MO): Elsevier; 2011. 224 p.

41. Young AN, du Plessis WM, Rodriguez D, Beierschmidt A. Thoracic radiographic anatomy in vervet monkeys (*Chlorocebus sabaeus*). J Med Primatol. 2013;42:310–317.

42. Zwart PC. Contribution to the pathology of the red panda (*Ailurus fulgens*). In: Glatston AR (ed.). Red panda biology. The Hague (The Netherlands): SPB Academic Publishing; 1989. p. 25–29.

Received for publication 11 January 2016